Transactions, SMiRT-26
Berlin/Potsdam, Germany, July 10-15, 2022
Division V

VERTICAL LOAD CAPACITY AND COLLAPSE BEHAVIOR OF REINFORCED CONCRETE MEMBERS WITH SHEAR FAILURE

Yoshinori Miyagawa[1] , Satoshi Komatsu[2]

[1] Senior research scientist, Central research institute of electric power industry, Japan (miyagawa@criepi.denken.or.jp)
[2] Research scientist, Central research institute of electric power industry, Japan

ABSTRACT

The vertical load bearing mechanism and collapse behavior after shear failure of reinforced concrete plane members with low axial stress and low out-of-plane shear reinforcement were investigated. The experiment was conducted with a dedicated loading apparatus that made the specimens collapse under the weight of steel ingots following severe damage by horizontal load. Collapse occurred not simultaneously with shear failure but after the apparent thickness increased more than the maximum experience value of relative displacement between both ends. The progress of the downward displacement of the top slab could be classified into several phases that include slight sinking just after shear failure and drastic sinking accompanied by rebar buckling. Resistance against collapse was improved when the side of the specimen was restrained by sand or the core concrete was not damaged due to the precedence of bond splitting failure.

INTRODUCTION

The target of the present research is underground structures, such as water channels and plumbing tunnels, which are involved in the cooling of nuclear reactors in an emergency. These structures are required to be impervious to collapse and provide cooling water to emergency equipment during and after earthquakes. They are surrounded by ground and their cross section often has a rigid frame structure. Despite the fact that such characteristics make them statically indeterminate and redundant, the criteria in performance verification are decided with reference to their horizontal load bearing capacity limit. Elucidation of the structural behavior of such structures until loss of their interior space is necessary for more rational evaluation. The target structures have axial stress ratio of 0 to 0.1 and tensile reinforcement ratio between approximately 0.2% and 0.7%. Their members are often less or not reinforced in the out-of-plane direction when the construction age is old. These characteristics tend to result in their failure mode being out-of-plane shear failure after flexural yielding. From the point of collapse resistance, low axial stress ratio is an advantageous condition whereas low out-of-plane shear reinforcement is disadvantageous.

PREVIOUS RESEARCH

A number of previous research works focused on collapse or vertical load capacity after shear failure. Yoshimura et al. (2005) proposed an evaluation method of horizontal and vertical displacement at collapse for the members to fail in shear mode. Failure surface was introduced as the conceptual extension of yield surface in plastic mechanics and vertical and horizontal displacement were viewed as linked to each other based on the idea that the failure surface shrinks after shear failure. Elwood and Moehle (2005) derived the vertical load capacity after shear failure based on a shear friction model where shear transfer across a crack is likened to friction. Parra-Montesinos et al. (2006) mentioned that the collapse of the Daikai subway

station in the 1995 Hyogoken-Nanbu earthquake was reasonably reproduced by the application of the shear friction model. Kato et al. (2006), (2007) also proposed a formula to evaluate horizontal displacement at collapse based on a systematic experiment.

However, even in these cases, the presence of some shear reinforcement has been a prerequisite. When the proposed formulae or methods are applied to members without transverse rebars, either the solution is the constant low limit value or not available beyond the scope. Therefore, we planned the experiment concerning the collapse of members without shear reinforcement.

COLLAPSE TEST OF SINGLE WALLS AND BOX CULVERTS WITH SHEAR DAMAGE

Outline

A horizontal cyclic load was applied to reinforced concrete specimens carrying approximately 100 kN of weight. The phenomenon of the top part of the specimen losing its support and falling was observed and measured. The number of specimens was nine. The conditions of each case were arranged as shown in **Table 1**. The test parameters were specimen shape, axial stress ratio, loading method (static and cyclic/dynamic and cyclic/dynamic and monotonic), the presence/absence of lateral ground, and the presence/absence of out-of-plane shear reinforcement. This test was conducted in three groups in three years owing to the necessity of confirming the feasibility of the test apparatus step by step.

Table 1: Case list.

Case name	Specimen type	Axial stress [N/mm^2] (Axial stress ratio)	Loading method	Out-of-plane shear reinforcement	Lateral ground	Mortar (Alternative of concrete)			Horizontal load capacity (Cal.)			Test results	
						Compressive strength [N/mm^2]	Young's modulus [kN/mm^2]	Tensile strength [N/mm^2]	Shear strength (i) [kN]	Flexural strength (ii) [kN]	Ratio (i)/(ii)	Deformation angle at shear failure [rad]	Maximum load [kN]
S1	Single wall	0.766 (0.032)	Static Cyclic	-	-	23.6	25.8	1.88	57.1	65.3	0.87	0.010	69.6
S2	Single wall	1.624 (0.071)				23.0	25.7	1.79	61.9	71.9	0.86	0.007	80.8
S3	Box culvert	0.812 (0.034)				24.2	25.9	1.97	115.7	132.1	0.88	0.016	119.9
DA1	Single wall	0.804 (0.027)	Dynamic Cyclic			29.7	24.2	2.35	62.2	63.6	0.98	0.018	64.8
DA2	Single wall	1.687 (0.056)				30.3	24.6	2.30	68.4	71.4	0.96	0.023	79.2
DA3	Box culvert	0.843 (0.027)				30.7	25.0	2.26	126.2	128.4	0.98	0.025	106.8
DBG	Box culvert	0.843 (0.023)			○	36.4	29.3	2.34	135.2	115.8	1.17	0.021	157.9
DBW	Single wall	1.687 (0.046)		0.22%	-	36.5	28.1	2.43	129.2	65.7	1.97	0.023	84.3
DBM	Single wall	1.687 (0.046)	Dynamic, Monotonic	-		36.7	26.8	2.52	74.0	65.7	1.13	0.030	92.5

Specimen and Test Apparatus

The shape, dimensions, and rebar arrangement of the specimens are shown in **Figure 1**. The specimen shape was of two types: a single wall, and a one-span box culvert with two walls. The horizontal load was applied in the out-of-plane direction, which corresponds to the deformation of the tunnel cross section. Both types of specimens had 600 mm depth, 100 mm thickness, and 16 mm cover depth to the center of the rebar. Mortar with 5 mm of maximum coarse aggregate diameter was used as the matrix and stainless-steel (SUS304) screw rods of M3 thread size were used as main bars in consideration of the reduced scale. The tensile reinforcement ratio was 0.39% based on the effective sectional area of the screw rods. Steel wires (SWRCH10R) with 2.6 mm diameter, the amount of which was equivalent to 0.22% in transverse reinforcement ratio, were arranged as out-of-plane shear reinforcement only for the DBW case. Haunches were not reinforced by oblique bars.

Figure 2 depicts the test apparatus for the dynamic loading cases. The table below the specimen was supported by linear bearings and it could move in the horizontal direction with little resistance. On the other hand, the reaction block was positioned above the specimen and it also served as the table for the steel ingots. The reaction block was connected to the triangular steel walls with vertical linear bearings in between.

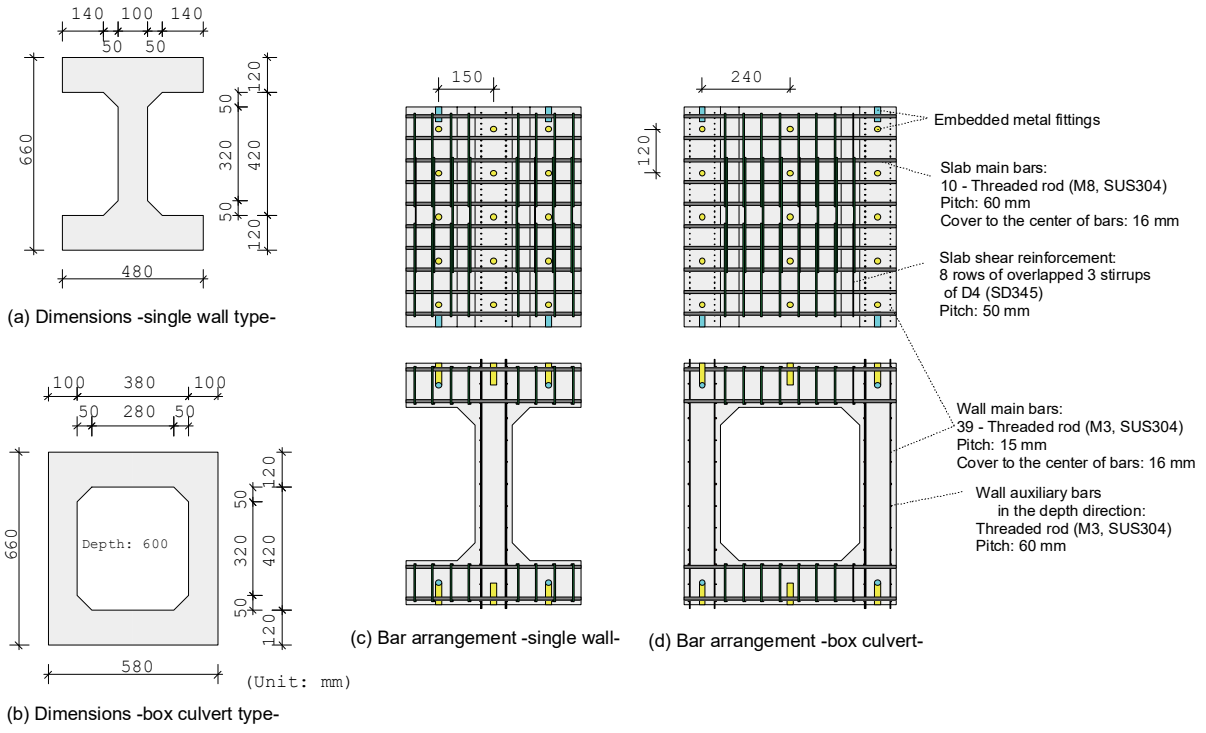

Figure 1. Dimensions and rebar arrangement of specimens.

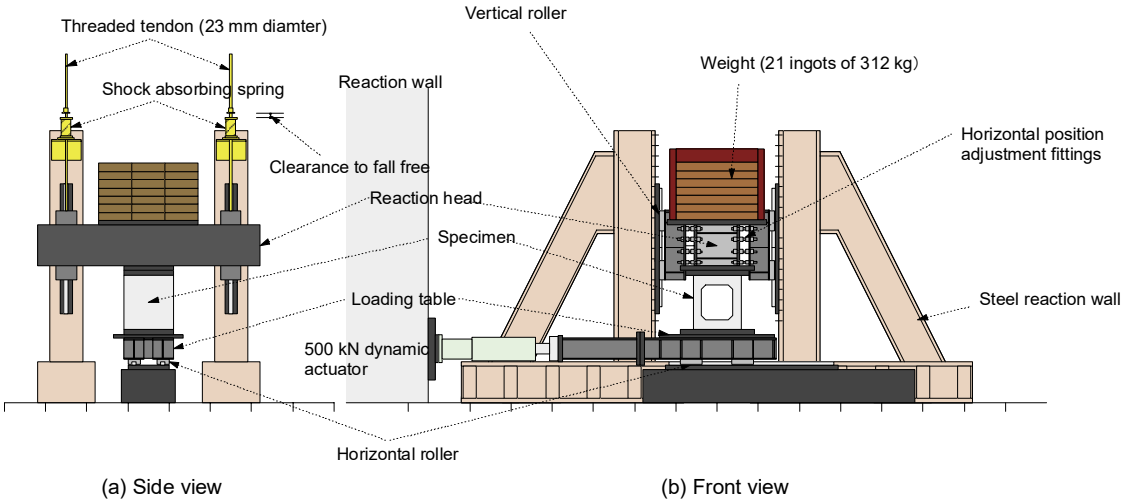

Figure 2. Test apparatus (configuration for dynamic loading cases).

Accordingly, the upper end of the specimen was constrained against horizontal displacement and rotation and free for vertical movement. When the damage of a specimen due to horizontal loading becomes sufficiently severe, the reaction block with the steel ingots loses its support and falls freely. The magnitude of the vertical load was controlled by the number of ingots put on the reaction block. The total mass including the reaction block, the vertical linear bearings and all the ingots was 10.328 t. The horizontal displacement of the lower table was controlled by hydraulic jacks. Regarding the three static loading cases tested earlier, 200 kN push-only jacks were installed on both sides of the table. This first apparatus was found to be problematic owing to the fact that it could lose control temporarily just after the event of a shear failure or collapse. Thus, the 200 kN push-only jacks were replaced by ±500 kN servo control actuators

from the second group i.e., the dynamic loading cases. The DBG case was prepared to simulate the side constraint by ground. A soil tank was constructed with 30 mm thick acrylic boards and steel frames, as shown in **Figure 3**. Note that the tank did not have a device to cause deformation according to horizontal loading as a limiting condition. Both side spaces between the specimen and the tank were filled with dry sand to the depth of 600 mm.

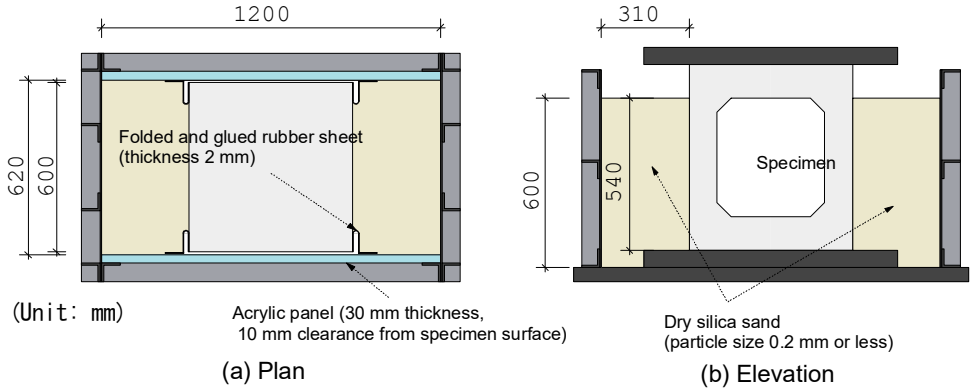

Figure 3. Soil tank and sand arrangement in DBG case.

Table 2: Rebar properties.

Case name	Role	Effective area or Nominal area [mm^2]	Young's modulus [kN/mm^2]	Yield strength** [N/mm^2]	Tensile strength [N/mm^2]
S1-S3	Main reinforcement	5.03	178.3	600.3	866.0
DA1-DA3	Main reinforcement	5.03	181.3	465.5	751.4
DBG, DBW, DBM	Main reinforcement	5.03	169.7	379.4	668.0
DBW	Out-of-plane reinforcement	5.22*	205.4	579.4	632.6

*Measured value **0.02% offset value

The mechanical properties of the mortar of each specimen have shown in **Table 1**. It must be noted that the above-mentioned schedule brought about different material properties for each of the S, DA, and DB groups. **Table 2** shows the tensile property of the rebar. The rebar did not have an articulate yielding plateau and the stress-strain skeleton was well approximated by the Menegotto-Pinto curve. The steel wires used in the DBW specimen were extremely brittle material that broke in tensile strain of 4000 to 6000 micro. Shear strength, flexural strength, and the ratio between them are also listed in **Table 1**. Flexural strength was calculated based on the Navier-Bernoulli hypothesis, and shear strength was derived from the formula adopted in the Japanese standard for civil engineering structures (Niwa et al., 1986).

The lateral constraint in the DBG case was formed with No. 7 silica sand (particle size 0.2 mm or less). The actual density in the soil tank was 1.53 t/m3 (relative density 100%). The horizontal resistance of the filled sand was investigated separately by the partial test to prevent unfavorable damage to the main specimen. The same tank and a steel plate in which soil pressure gauges were embedded were used for that test. **Figure 4(a)** displays the relationship between the deformation angle of the pressure receiving plate and the total horizontal load transferred to the sand. The value of the vertical axis is the summation of the four gauges when the interval of 0.1 m was assumed to be the assigned depth for each gauge. Although the ground depth was very shallow, the horizontal load of 40 kN to 50 kN could be transferred in the deformation angle of 2%. **Figure 4(b)** shows the soil pressure distribution in the vertical direction at the representative timepoint. The soil pressure was relatively small around the lower end pin and the ground surface, and large in the middle section with 0.2 to 0.3 m depth.

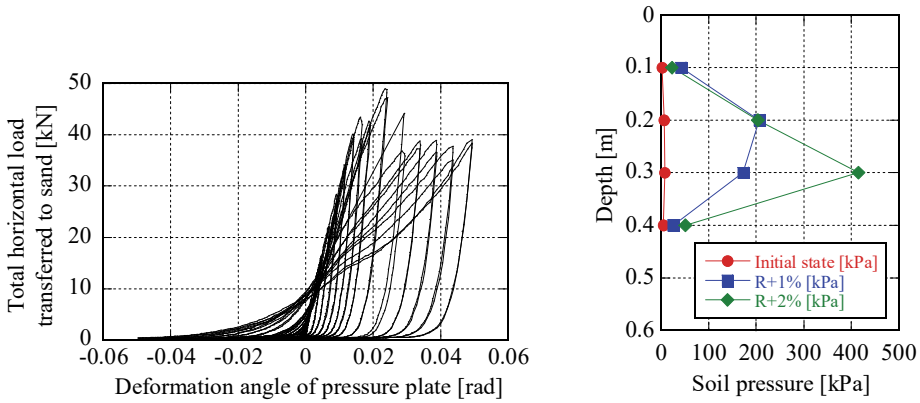

(a) Total horizontal load transferred to sand (b) Soil pressure distribution

Figure 4. Result of partial test for sand on the side.

Measurement and Loading Schedule

Point measurement by displacement transducers and accelerometers, and two-dimensional image measurement with the markers stuck to the specimen surface in a grid pattern, were combined. Regarding the static S group, the data during horizontal loading was recorded statically and time history recording with a dynamic logger was added only for the moment of collapse. The images for measurement were taken with a commercially supplied single-lens reflex camera (resolution of 4254×2836 pixels) at intervals of five seconds. For the dynamic DA and DB groups, the images were taken with a high-speed camera. It was set to take 6548 images with 1920×1080 pixel of resolution at intervals of one thousandth of a second when a trigger signal was generated once.

Table 3: Wave list.

Sequence ID	Amplitude (story drift R) [rad]	Frequency [Hz]	Velocity [cm/s]
a	0.0010	2.00	0.68
b	0.0020		1.36
c	0.0050		3.39
d	0.0075		5.09
e	0.0100		6.79
f	0.0125		8.48

Sequence ID	Amplitude (story drift R) [rad]	Frequency [Hz]	Velocity [cm/s]	Test result (Failure event)	
				Shear failure	Critical sinking
g	0.0150	1.96	10.00		
h	0.0175	1.68			
i	0.0200	1.47		DA1	
j	0.0250	1.18		DA2	DA2
k	0.0300	0.98		DA3, DBG, DBW	DA1, DA3, DBW
l	0.0350	0.84			
m	0.0400	0.74			
n	0.0450	0.65			DBG

In describing the loading schedule, the letter R is used to express the control displacement divided by 540 mm as the distance between the center levels of the top and bottom slabs. The horizontal load in the static cases was applied three times cyclically turning at R±0.1%, 0.2%, 0.5%, 0.75%, 1.0%, 1.5%, 2.0%, and 2.5%, except for the subsequent large deformation stage. On the other hand, the displacement sequence of sine waves where three magnifying waves, five steady waves, and three decreasing waves were contained was given in the dynamic cases. The maximum amplitude of the sequence was increased step by step, as shown in **Table 3**. The frequency had been fixed to 2 Hz while the maximum amplitude was small, but it was reduced gradually in the latter large amplitude stage because the actuator had the upper limit of 100 mm/s for velocity. After shear failure occurred, the sequence with the same maximum amplitude was repeated four times to confirm the influence of repetition on the post-peak behavior. The loading speed for DBM, the only monotonic loading case, was determined as 43.2 mm/s.

TEST RESULTS AND DISCUSSION

The common characteristic results found through all cases were mentioned before the detailed discussion. The first observable damage was flexural cracks at both ends of the vertical members. Subsequently, shear cracks at an angle of 45 degrees to the member axis were induced in section 1D (D means thickness) away from the ends. Nevertheless, these initial oblique cracks did not trigger a reduction in horizontal load capacity because a second shear resistance mechanism with concrete strut having a lower angle than 45 degrees was formed. After horizontal loading was continued, a shear crack with a lower angle than 45 degrees was generated nearer to the center of the member. Shear failure in the following text basically refers to the occurrence of this second oblique crack, which induced a reduction in horizontal load capacity. Collapse did not occur at the same time as shear failure in any case. There was some time lag even in the two cases of DA2 and DBW, in which collapse occurred during the same vibration sequence as shear failure. Moreover, horizontal load capacity had been almost completely lost at the timepoint of collapse.

Behavior before Shear Failure

Figure 5 shows the relationship between horizontal displacement and horizontal load for all cases. The only skeleton curves were drawn in the figure to ensure visibility because there are a lot of inner hysteresis curves especially for the dynamic cases.

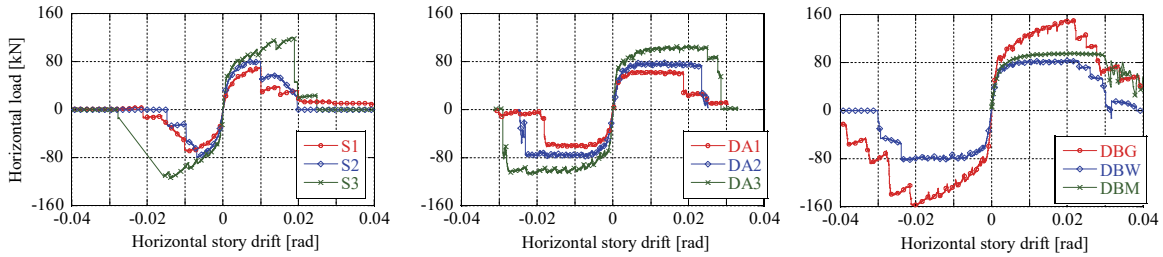

(a) S1-S3 (b) DA1-DA3 (c) DBG,DBW,DBM

Figure 5. Skeleton curves of the relationship between horizontal displacement and horizontal load.

The specimens belonging to the DA group exhibited deformation performance superior to that of the S group. This tendency is presumed to be the influence of the material property rather than loading speed. Because the specimens of the S group had low compressive strength of mortar and high tensile strength of reinforcement, they revealed the characteristic as shear member to a greater extent.

The horizontal load capacity of the culvert-type specimens, S3 and DA3, did not reach the double value of the single wall specimens S1 and DA1. Whereas single wall specimens have haunches on both surfaces, the haunch in each wall of the culvert specimens is arranged on the inner surface only. Accordingly, the substantial length of the vertical members of the culvert specimens was greater than that of the single wall specimens. The same reason is given for the fact that horizontal displacement at the time of shear failure was larger in the culvert specimens.

The horizontal load capacity of DBG was noticeably large because the force transferred to the sand was included. The horizontal displacement at shear failure of DBW was not much different from that of DA2, although the softening gradient became rather gentle. Typically, shear reinforcement improves member ductility. However, this effect was quite limited in DBW. The poor bond of the steel wires with a smooth surface made the width of oblique cracks increase enough to lose aggregate interlock. Moreover, the lack of ductility did not allow them to bear the stress concentrated in them.

The first reduction of horizontal load capacity in the monotonic DBM case occurred at the horizontal story drift of 0.03, which was not much different from the other specimens loaded cyclically. Nevertheless, bond splitting cracks along the main bars were observed instead of oblique cracks only in this

case. The load capacity from the aspect of bending moment had been held constant although the horizontal load was reduced due to a geometric effect.

Progressive Sinking Phase from Shear Failure to Collapse

Organizing the test results, four phases are recognized regarding the sinking from shear failure to collapse. Firstly, slight sinking was caused at shear failure in many cases. However, the amount of sinking was in the small range of 0.1 mm to 1 mm. Secondly, there was a phase of gradual sinking progress with the continued horizontal loading. This was considered to reflect the elongation of existing cracks or the deterioration of crack surfaces. This phase continued to the end of the test in the DBG case in particular (**Figure 6(c)**). In the third phase, the upper part of the specimen became unstable suddenly and sank remarkably over 10 mm. This was accompanied by buckling of the main bars. Classified further, there were cases where the specimen recovered stability after sinking to some extent, namely S1, S3, DA1, and DBW,

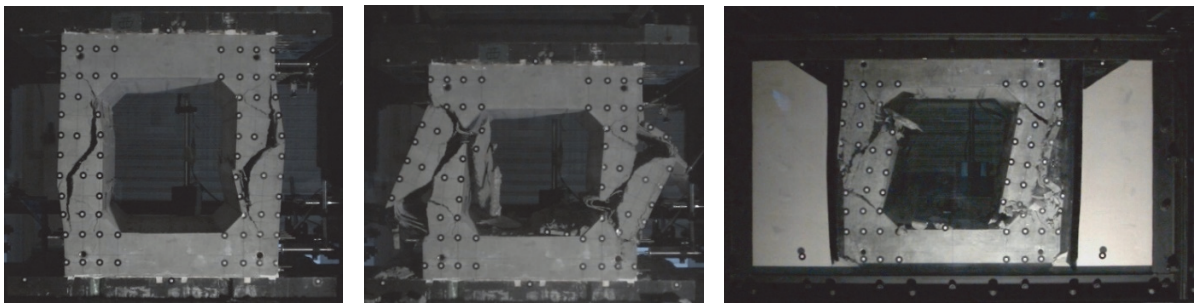

(a) DA3 (before critical sinking) (b) DA3 (after critical sinking) (c) DBG (at the end of test)

Figure 6. Snapshot before and after collapse.

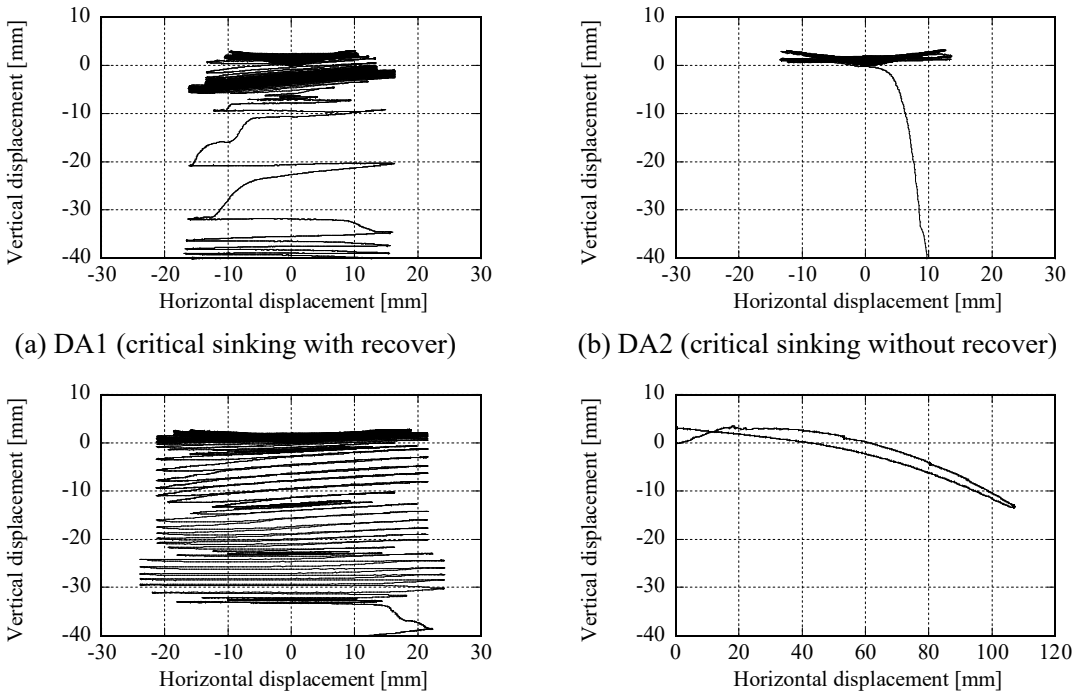

(a) DA1 (critical sinking with recover) (b) DA2 (critical sinking without recover)

(c) DBG (gradual sinking) (d) DBM (geometrical sinking)

Figure 7. Orbit between horizontal displacement and vertical displacement.

and other cases where the specimen lost stability completely, namely S2, DA2, and DA3 (**Figure 6(a), (b)**). Note that this phase is referred to as critical sinking hereafter. Finally, the downward displacement could be generated geometrically in the large horizontal displacement such as the DBM case. The relationship between horizontal and vertical displacement of the typical cases for each phase is represented in **Figure 7**.

Apparent Thickness Expansion Due to Shear Crack Opening

Displacement distribution in members varied outstandingly before and after shear failure. As shown in **Figure 8(a)**, the rotation of plastic hinges has larger contribution to the relative displacement between the top and bottom ends before shear failure. On the other hand, apparent thickness increases around an oblique crack after shear failure, and the upper and lower blocks of concrete are unloaded and their elastic deformation disappears. The thickness increment around an oblique crack and the horizontal displacement of the upper end should be almost the same under the idealized state shown in **Figure 8(b)**. Based on this assumption, the maximum value of thickness increment along the member axis, which was obtained through image measurement just before the critical sinking, was compared with the maximum experienced horizontal displacement in **Table 4**. The thickness increment value in the table is a simple subtraction of the length in the horizontal direction with reference to the initial state. As a side note, the Euclidean distance between the two referred points does not differ much. The data of the timepoint when the vertical acceleration of the loading head indicated a negative value were selected for the dynamic loading cases.

The thickness increment was larger than the maximum experienced horizontal displacement except for DBM. Moreover, it was less than the sum of the absolute value of the maximum experienced horizontal displacement in both directions in many cases. This range of thickness increment could be interpreted as the contribution of cyclic loading in both directions. As for DBM, although bond splitting cracks also contributed to a moderate increase in thickness, it was held even in the large horizontal displacement.

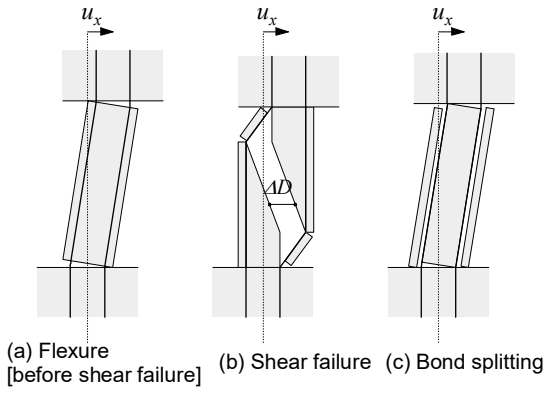

Figure 8. Typical variation of displacement distribution before and after shear failure.

Table 4: Deformation just before critical sinking.

Case name		Thickness increment just [mm]	Maximum experienced horizontal displacement [mm]	
			Large absolute value, + or -	Sum of absolute values of both directions
S1		11.4	11.5	22.5
S2		11.3	10.7	18.8
S3	Left wall	20.6	15.1	28.6
	Right wall	19.3		
DA1		24.2	16.4	32.6
DA2		22.3	13.5	26.9
DA3	Left wall	17.1	15.7	31.1
	Right wall	32.3		
DBG	Left wall	49.5	24.3	48.1
	Right wall	72.5		
DBW		28.6	16.0	32.0
DBM*	Horizontal displacement: 106.8 mm	16.4	106.8	106.8

*DBM did not reach 40 mm of sinking

Figure 9(a) shows the relationship between the thickness increment and the vertical displacement of the top of specimen S2. The state just before critical sinking is indicated by an arrow with the letter A and the coordinates are written next to it. The thickness increment before shear failure was approximately zero. The change in vertical displacement was small in the area from shear failure to point A despite the increase of the thickness increment. This means that the mortar block above the oblique crack was not sliding down along the crack surface but moving in the horizontal direction. **Figure 9(b)** shows the time transition of thickness increment and the vertical displacement of the top of specimen DA2. An oblique crack corresponding to shear failure occurred after a little over five seconds and the thickness increment

increased. However, the fluctuation of vertical displacement was limited again. The ratio of sinking to thickness increment was small in the other cases as well until critical sinking.

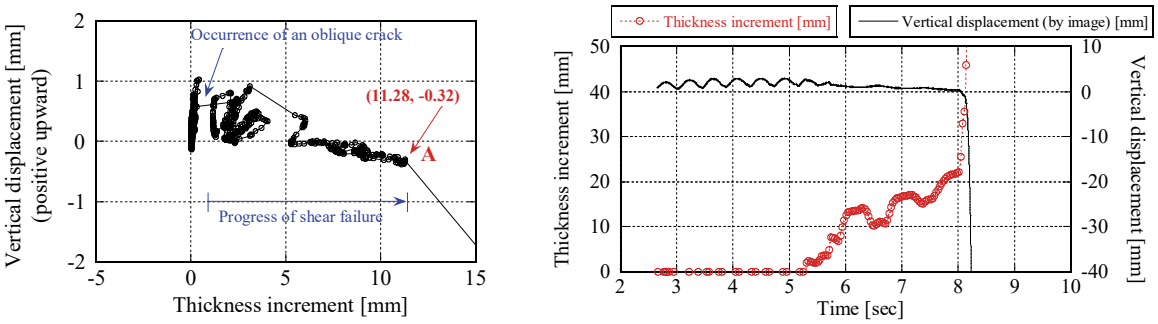

(a) S2 (b) DA2 (sequence j-1)

Figure 9. Transition of thickness increment and vertical displacement.

Buckling of Main Bars

The critical sinking was always accompanied by buckling of the main bars. The five bending patterns observed during the test are described as follows and are shown in **Figure 10**.

(i) The main bars buckle over the length of the member and the cover mortar spalls off in the same area.

(ii) The main bars buckle over the length of the member and the mortar including the core part juts out.

(iii) Buckling of the main bars and spalling of the cover mortar occur in the limited range between a member end and the end of an oblique crack.

(iv) Buckling of the main bars occurs in the very short range around a member end. The bars slip out from the vicinity of an oblique crack and they are bent until the axes become parallel to the inclined surface of the haunch.

(v) The main bars buckle not toward the near surface but toward the far surface.

The result of each specimen is classified into these patterns in **Table 5**. When the content of the table is collated with the above-mentioned sinking phases, the cases where stability was recovered after critical sinking (S1, S3, DA1, DBW) include pattern (iv). The extreme kinking bars in pattern (iv) resisted

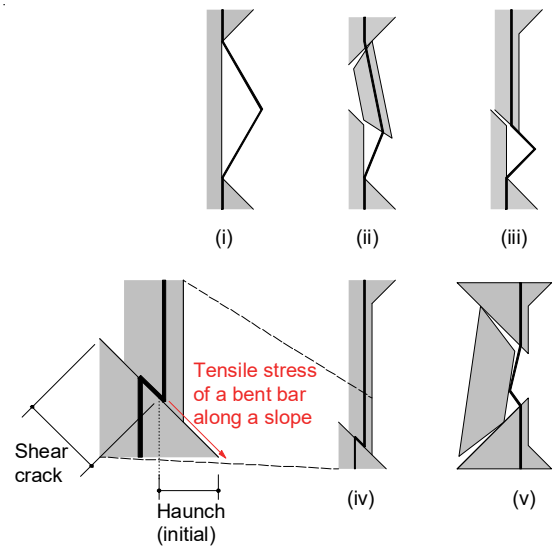

Figure 10. Observed buckling patterns of main bars.

Table 5: Classification of buckling pattern.

Case name	Single wall or left wall of box culvert		Right wall of box culvert	
	Left row (outer)	Right row (inner)	Left row (inner)	Right row (outer)
S1	i	iv		
S2	i	i		
S3	i	iv	iv	i
DA1	iv	i		
DA2	ii	i		
DA3	ii	iii	iii	ii
DBG*	-	ii	iv	v
DBW	iv	iii		
DBM	i	i		

*Buckling was not observed in the outer row of the left wall.

against the motion of the upper mortar block to slip down along the slope that was formed by the connection of the oblique crack surface and the haunch surface. When the vertical component of the tensile strength is calculated assuming the bars subjected to tension down 45 degrees, the summation of one rebar layer (39 bars) reaches 92.7 kN to 120.1 kN. This means that the bent rebars alone could support the vertical load to a sufficient extent. Pattern (v) is peculiar to the DBG case and appeared as the result of the lateral constraint by sand suppressing buckling toward the outer surface.

SUMMARY

The behavior of reinforced concrete members with low axial stress and low shear reinforcement in the collapse after shear failure was investigated experimentally. As a result, the following findings were obtained.

(1) Collapse occurred not simultaneously with shear failure but after the specimen lost most of its horizontal load capacity and the thickness increment exceeded the maximum experience value of relative displacement between both ends.
(2) The negative influence of the increasing axial stress and of loading speed on deformation performance was unremarkable in the present scope (axial stress ratio of 0.023 to 0.071).
(3) The fluctuation of vertical displacement was small from shear failure to critical sinking. This means that the upper part of an oblique crack did not slide down along its inclined surface but moved horizontally.
(4) When lateral restraint was given with dry sand, the progress of sinking due to horizontal loading was significantly reduced.
(5) In the monotonic loading case, bond splitting was so dominant that this prevented core concrete from inducing an oblique crack. Vertical displacement progressed only as the result of geometrical deformation because the core remained sound.
(6) When main bars buckled in the short range near a haunch, a mechanism whereby the main bars bent 135 degrees along the haunch resisted collapse through tension was formed. Stability was recovered on this occasion even after critical sinking was caused once.

REFERENCES

Elwood, K. J., and Moehle, J. P. (2005). “Axial capacity for shear-damaged columns,” *ACI Structural Journal*, Vol.102, No.4, pp.578-587

Kato, D., Li, Z., Nakamura, Y. and Honda, Y. (2006). “Tests on Axial Load Capacity of Shear Failing R/C Columns Considering Reinforcing Details - Relationship between Axial Loading Test and Lateral Loading Test -,” *J. Struct. Constr. Eng.*, AIJ, No.610, pp.153-159

Kato, D., Li, Z., Nakamura, Y. and Honda, Y. (2007). “Study on Evaluating Method of Axial Load Capacity of Shear Failing R/C Columns Considering Reinforcing Details,” *J. Struct. Constr. Eng.*, AIJ, No.616, pp.173-178

Niwa, J., Yamada, K., Yokozawa, K. and Okamura, H. (1986). “Revaluation of the Equation for Shear Strength of Reinforced Concrete Beams without Web Reinforcement,” *Proc. of JSCE*, No.372/V-5, pp.167-176

Nuclear Civil Engineering Committee, JSCE (2018). Safety Evaluation Manual for Earthquake Resistant Design of Important Civil Engineering Structures in Nuclear Power Plants 2018

Parra-Montesinos, G. J., Bobet, A., and Ramirez, J. A. (2006). “Evaluation of Soil-Structure Interaction and Structural Collapse in Daikai Subway Station During Kobe Earthquake,” *ACI Structural Journal*, pp.113-122

Yoshimura, M. and Takaine, Y. (2005). “Evaluation of Vertical Deformation for R/C Columns with Shear Mode Based on Concept of Failure Surface Contraction,” *J. Struct. Constr. Eng.*, AIJ, No.592, pp.167-175